



Tropospheric Water Vapor Anomalies During the 2006-07 and 2009-10 El Niños

Hanik Takahashi¹, Hui Su², Jonathan H. Jiang², Z. Johnny Luo³, Shang-Ping Xie^{4,5}, Jan Hafner⁵

¹Program in Earth and Environmental Sciences, Graduate Center, CUNY, New York, New York, USA.

²Jet Propulsion Laboratory, California Institute of Technology, Pasadena, California, USA.

³Department of Earth and Atmospheric Sciences and NOAA-CREST Center, City College of New York, CUNY, New York, New York, USA.

⁴Scripps Institution of Oceanography, University of California at San Diego, La Jolla, California, USA.

⁵International Pacific Research Center, and Department of Meteorology, SOEST, University of Hawaii at Manoa, Honolulu, Hawaii, USA



Abstract

Water vapor measurements from the Aura Microwave Limb Sounder (MLS) and Aqua Atmospheric Infrared Sounder (AIRS) are analyzed to study the variations of moisture during the 2006-07 (East Pacific El Niño) and 2009-10 El Niños (Central Pacific El Niño or El Niño *Modoki*). Results show that these two types of El Niño events produce different patterns of water vapor anomalies over the tropical ocean, which approximately resemble those of cloud anomalies shown in *Su and Jiang* [2012]. The principal findings of the study are as follows: (1) A clear "upper tropospheric amplification" of the fractional water vapor change to El Niño is found from regression analysis of water vapor on the Niño-3.4 SST. (2) Water vapor anomalies are mostly controlled by the thermodynamic factor during the 2006-07 El Niño, but they are sensitive to both dynamic and thermodynamic changes during the 2009-10 El Niño. (3) GFDL AM2.1. model simulates the general patterns of water vapor response to the ENSO SST forcing; however, it does not reproduce the strong moistening effect at 200 hPa where convective detrainment preferably occurs. (4) The water vapor distributions sorted by large-scale regimes are very different during the 2009-10 El Niño owing to critical simulation errors over the Indian Ocean.

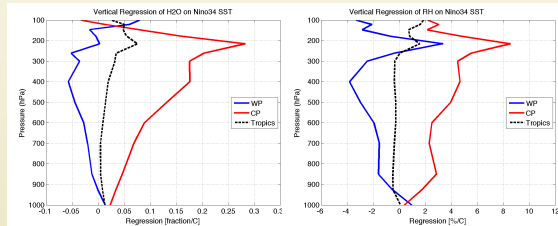
Data and Methodology

In this study, AIRS (below 300 hPa) and MLS (above 300 hPa) data from 2004-2011 are used over the tropical ocean together with GFDL AM2.1. simulation for the period of 2005-2012.

- AIRS footprint is approximately 13.5 km at nadir. We use AIRS version 5, Level 3 H₂O product AIRXSTD whose spatial resolution is 50 km, but aggregated on 1°×1° (longitude × latitude) grid.
- The vertical resolutions of water vapor from MLS are ~2.5 km at 316-215 hPa, ~3.0 km at 100-1.0 hPa, and >3.4 km at levels higher than 1.0 hPa and its retrievals are horizontally spaced by 165 km.
- GFDL AM2.1. is an atmosphere-only model forced by observed SSTs. The horizontal resolution is 2.5°×2° (longitude × latitude). It has 24 vertical levels: the lowest level is about 30 m above the surface, nine full levels are in the lowest 1.5 km above the surface, and five levels are in the stratosphere with the highest level at about 3 hPa.

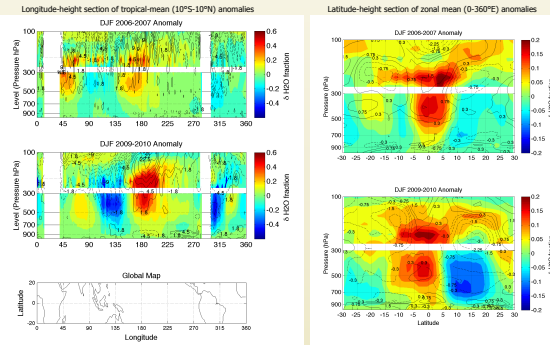
1. Regression Analysis of Water Vapor on the Niño-3.4. SST

- The regression of water vapor anomalies onto the Niño-3.4 SST is analyzed, revealing a clear "upper tropospheric amplification" of the fractional water vapor change to El Niño.
- The increase rate of water vapor with Niño-3.4 SST is the highest around 200 hPa (0.28/C) over the central Pacific where the largest convective anomalies are observed.



2a. Zonal and Meridional Structure of Water Vapor Anomalies

- These two types of El Niño events produce different patterns of water vapor anomalies in the tropical ocean, which resemble those of cloud anomalies.
- The anomalous drying over the northern hemisphere is observed during 2009-10 El Niño and it is thought to be due to the acceleration of the winter Hadley cell.



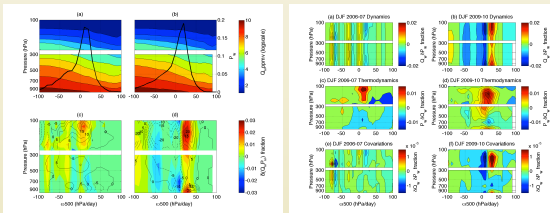
2b. Water Vapor Anomalies Sorted by Large-scale Circulation

Following *Bony et al* [2004], ω_{500} (mid-tropospheric vertical pressure velocity at 500 hPa) is used as a proxy of local dynamic condition, and water vapor is treated as a function of ω_{500} weighted by the probability density function of each ω_{500} regime. Following is the equation we use:

$$\delta(Q_{\omega}, P_{\omega}) = Q_{\omega} \cdot \delta P_{\omega} + P_{\omega} \cdot \delta Q_{\omega} + \delta Q_{\omega} \cdot \delta P_{\omega}$$

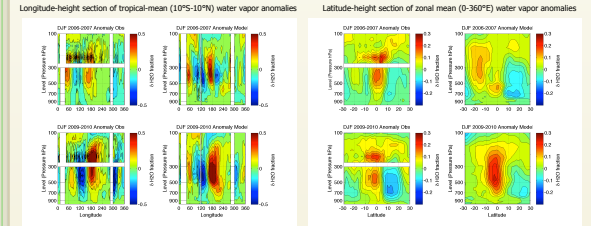
where Q_{ω} is the water vapor in a regime of the value ω and P_{ω} is the probability distribution function of the regime ω .

- Water vapor response to the 2006-07 El Niño is mainly forced by changes in thermodynamic structure of the atmosphere, while water vapor response to the 2009-10 El Niño is forced by both thermodynamic and large-scale circulation changes.

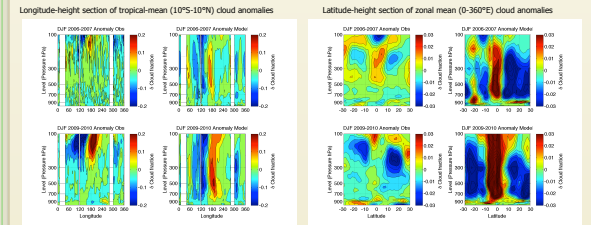


3. Comparison between Satellite Observation and GFDL Model Simulation

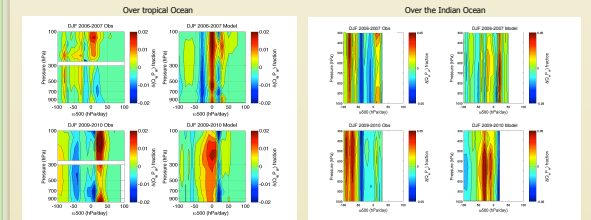
- GFDL AM2.1. does not reproduce the strong moistening effect at 200 hPa where convective detrainment preferably occurs, suggesting that these might be model deficiencies simulating realistic convective processes that moistening and drying the atmosphere.



- The strong acceleration bias of the Hadley Circulation is found in GFDL AM2.1., which has produced extremely high amounts of CFr over deep tropics, especially during the 2009-10 El Niño.



- The water vapor distributions sorted by large-scale regimes are very different during the 2009-10 El Niño owing to critical simulation errors over the Indian Ocean.



Reference and Acknowledgments

Bony, S., J.-L. Dufresne, H. Le Treut, J.-J. Morcrette, and C. Senior (2004), On dynamic and thermodynamic components of cloud changes. *Climate Dynamics* 22, pp. 71-86.

Su, H., and J.H. Jiang (2012), Tropical Clouds and Circulation Changes During the 2006-07 and 2009-10 El Niños, *J. Climate*, in press.

HT acknowledges the JPL Graduate Fellowship program. The work was conducted at the Jet Propulsion Laboratory, California Institute of Technology, under contract with NASA. HS and JHJ thank the funding support from NASA NEWS program. ZJL acknowledges funding support from the CloudSat-CALIPSO Science Team. SPX is supported by NSF and NOAA.